ELSEVIER

Materials Science and Engineering B94 (2002) 159–163

MATERIALS SCIENCE & ENGINEERING B

www.elsevier.com/locate/mseb

# Characterization of Ni-implanted GaN and SiC

S.J. Pearton [a,*], N. Theodoropoulou [b], M.E. Overberg [a], C.R. Abernathy [a], A.F. Hebard [b], S.N.G. Chu [c], R.G. Wilson [d], J.M. Zavada [e]

[a] *Department of Materials Science and Engineering, University of Florida, P.O. Box 116400, 100 Rhines Hall, Gainesville, FL 32611-6400, USA*
[b] *Department of Physics, University of Florida, Gainesville, FL 32611, USA*
[c] *Agere Systems, Murray Hill, NJ 07974, USA*
[d] *Stevenson Ranch, CA 91381, USA*
[e] *Army Research Office, Research Triangle Park, NC 27709, USA*

Received 12 June 2001; accepted 11 December 2001

**Abstract**

High concentrations ($>10^{21}$ cm$^{-3}$) of Ni were introduced into GaN and SiC by ion implantation at 350 °C. On subsequent annealing at 700 °C, there was more residual lattice damage in GaN compared to SiC. Both materials showed ferromagnetism with transition temperatures below 50 K. No secondary phases could be detected by transmission electron microscopy (TEM) or selected area diffraction in either GaN or SiC. The direct implantation process appears useful for studying ion/substrate combinations for potential spintronic applications. 

*Keywords:* Magnetic ions; Ferromagnetism; Ni

## 1. Introduction

Currently, there is a great deal of interest in the incorporation of magnetic ions into semiconductors to produce ferromagnetism. To date, the most studied systems have been (In, Mn)As and (Ga,Mn)As, in which the ferromagnetism is carrier-induced [1–8]. This introduces the possibility of electric-field control of magnetism in semiconductors with technological applications in photonics and electronics and hence the possibility of integrating magnetic devices with detectors, control electronics and other entities [9]. A major drawback with the two materials systems mentioned above is the fact that their Curie temperatures are well below room temperature (about 35 K for (In,Mn)As and 105 K for (Ga,Mn)As) [1–3]. Recent calculations have suggested that wider bandgap semiconductors could have much higher transition temperatures, in particular GaN and ZnO [10]. In addition, Mn is not the only impurity of interest in these materials and the family of elements V, Cr, Fe, Ni and Co could also induce ferromagnetism under the right conditions [11]. We have previously found that Mn implanted into p-GaN produced ferromagnetic behavior at $<250$ K [12,13], while Fe displayed an apparent transition temperature of $\leq 175$ K. Similar experiments with Mn and Fe implantation into SiC, another technologically important wide bandgap semiconductor, led to paramagnetic behavior with the Mn and ferromagnetism at $\leq 125$ K with the Fe.

In this paper, we report on the structural and magnetic properties of Ni-implanted GaN and SiC. In both materials, the magnetization shows ferromagnetic contributions with transition temperatures $\leq 50$ K, suggesting that Ni-doping is not a promising approach for room-temperature magnetic semiconductors.

## 2. Experimental

The GaN layers were grown by metal organic chemical vapor deposition on c-plane $Al_2O_3$ substrates, and consisted of a 3 μm undoped buffer and 0.5 μm of $p$ (hole concentration $\sim 3\times10^{17}$ cm$^{-3}$)—GaN doped using $Cp_2Mg$. The 6H–SiC substrates were Al-doped ($p\sim10^{17}$ cm$^{-3}$) and were implanted into the Si-face. All

* Corresponding author. Tel.: +1-352-846-1086; fax: +1-352-846-1182.
*E-mail address:* spear@mse.ufl.edu (S.J. Pearton).

0921-5107/02/$ - see front matter 
PII: S0921-5107(02)00056-9

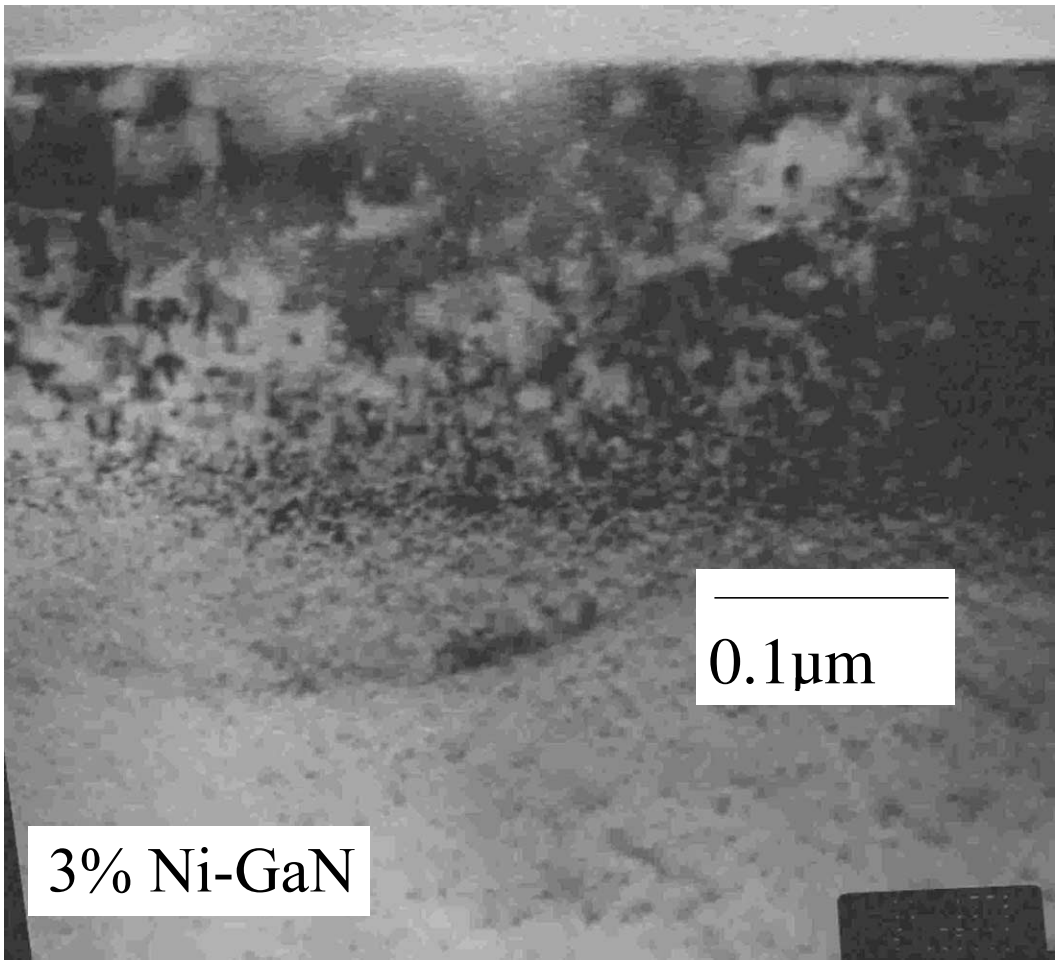


Fig. 1. TEM cross-section from GaN implanted with $3 \times 10^{16}$ cm$^{-2}$ $Ni^+$ at 250 keV and annealed at 700 °C.

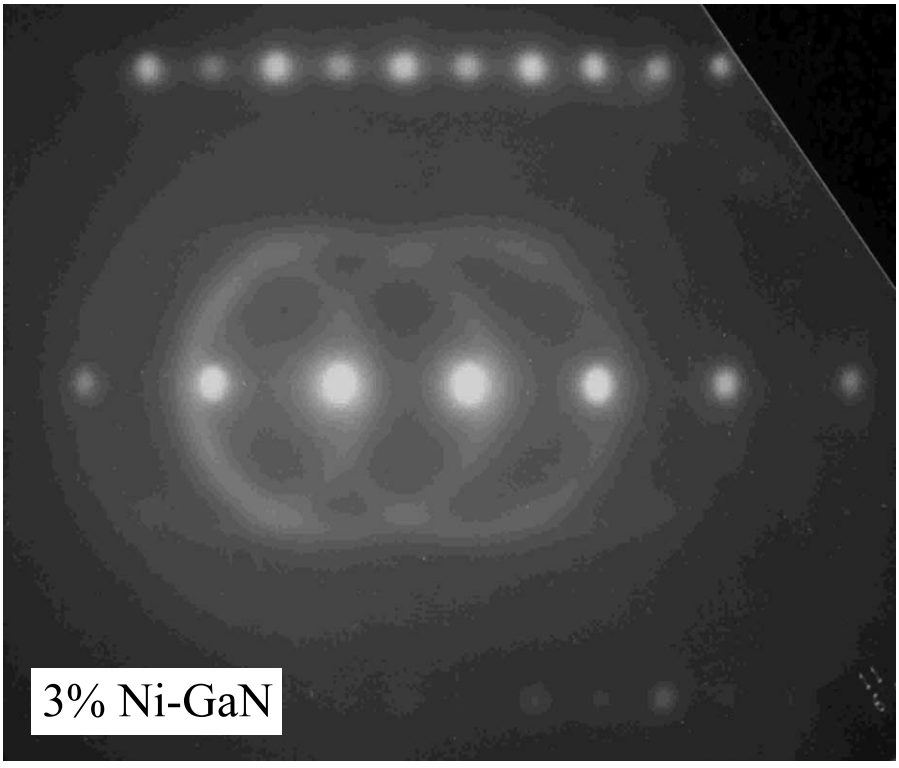


Fig. 2. Selected area diffraction pattern from Ni-implanted region of Fig. 1.

of the samples were held at ~350 °C during implantation to avoid amorphization [14]. Calculated ion profiles showed a projected range of ~200 nm for the 250 keV $Ni^+$ ions in both materials. The doses were varied from 3 to $5 \times 10^{16}$ $cm^{-2}$ at this fixed energy, leading to peak Ni concentrations corresponding to ~3–5 at.% at the projected range. The samples were annealed face-to-face at 700 °C for 5 min under a flowing $N_2$ ambient. The magnetic properties were measured in a Quantum Design SQUID magnetometer, while the structural properties were examined by transmission electron microscopy (TEM) and selected-area diffraction pattern (SADP) analysis.

## 3. Results and discussion

Fig. 1 shows a cross-sectional TEM micrograph of the 3 at.% Ni-implanted GaN. The damaged region is confined within a top surface layer ~0.24 μm thick. The residual damage after annealing consists of dislocation loops and other lattice defects, consistent with the previous reports [15–17]. We did not observe the platelet structures reported fin Mn-implanted GaN implanted at similar doses and annealed under the same conditions [12,13], which were ascribed to the formation of $Ga_xMn_{1-x}N$. Our experience with these high dose implants into GaN is that there is always significant residual damage after annealing, regardless of the annealing temperature. This is most likely related to the binary nature of the lattice and the inability to avoid formation of stable defect complexes.

The SADP shown in Fig. 2 reveals diffused rings with lattice constant slightly shorter than that of GaN along the *c*-axis (the radius of the ring in reciprocal space is slightly larger), which indicates that the Ni is being incorporated into the GaN lattice and shrinking it. The basic GaN diffraction spots in the implanted region are very strong and indicate that the lattice is basically intact. The rings are continuous because of double-diffraction from a surface amorphous region We expect that some fraction of Ni substitutes for Ga, in analogy with recent reports for Fe implanted into GaN [18]. Note that there is no evidence for secondary phase formation in the Ni-implanted GaN. Table 1(a) shows

Table 1
Potential phases found in Ni-implanted GaN and SiC

| Phase | Structure | a | b | c |
|---|---|---|---|---|
| (a) *GaNiN* | | | | |
| Ni | Cubic | 3.5238 | | |
| Ni | Hexagonal | 2.6515 | | 4.343 |
| $Ni_3N$ | Hexagonal | 4.621 | | 4.304 |
| $Ni_4N$ | Cubic | 3.745 | | |
| ϕ-$NiGa_4$ | Cubic | 8.4295 | | |
| $Ga_3Ni_5$ | Orthorhombic | 7.53 | 6.72 | 3.77 |
| $Ga_4Ni_3$ | Cubic | 11.411 | | |
| γ-$Ga_{1.4}Ni_{2.5}$ | Hexagonal | 4.000 | | 4.983 |
| β′-$Ga_3Ni_2$ | Hexagonal | 4.060 | | 4.897 |
| (b) *SiNiC* | | | | |
| NiSi | Orthorhombic | 5.233 | 3.258 | 5.659 |
| η-NiSi | Tetragonal | 7.6538 | | 8.4514 |
| $NiSi_2$ | Cubic | 5.416 | | |
| ?-$NiSi_2$ | Rhombohedral | 12.602 | | 15.277 |
| ?-$Ni_2Si$ | Hexagonal | 3.797 | | 4.8928 |
| d-$Ni_2Si$ | Orthorhombic | 7.39 | 9.90 | 7.03 |
| $Ni_3Si$ | Cubic | 3.5056 | | |
| $Ni_3Si$ | Monoclinic | 7.04 | 6.26 | 5.08 |
| $Ni_3Si_2$ | Orthorhombic | 12.229 | 10.805 | 6.924 |
| e-$Ni_3Si_2$ | Orthorhombic | 6.605 | 7.627 | 9.574 |
| ?-$Ni_5Si_2$ | Hexagonal | 7.6733 | | 9.7516 |
| $Ni_{31}Si_{12}$ | Hexagonal | 6.67 | | 12.28 |
| $Ni_{74}Si_{26}$ | Hexagonal | 6.698 | | 28.855 |
| NiC | Cubic | 3.539 | | |
| $NiC_x$ | Hexagonal | 6.171 | | 16.84 |
| $Ni_3C$ | Hexagonal | 2.651 | | 4.338 |
| $Ni_3C$ | Rhombohedral | 4.5828 | | 12.9916 |

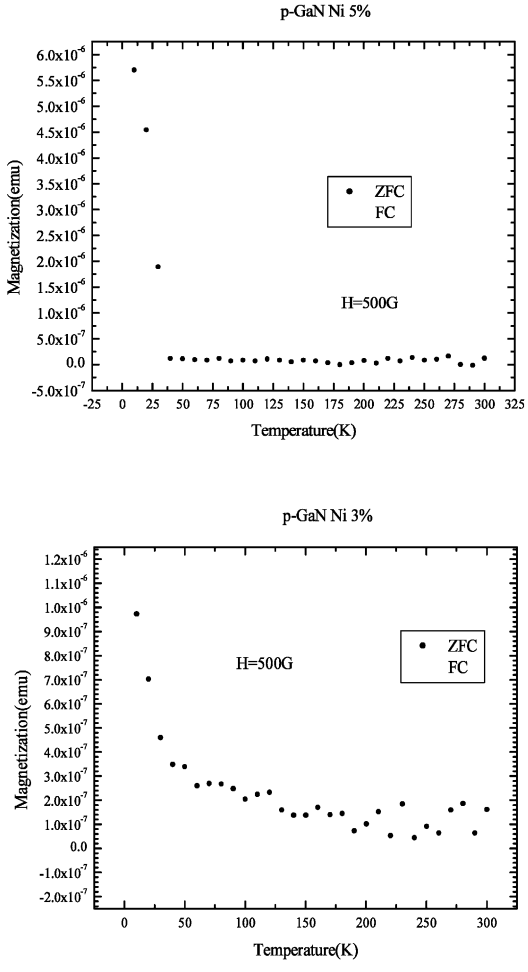


Fig. 3. Temperature dependence of difference between field-cooled and zero field-cooled magnetization from GaN implanted with either $5 \times 10^{16}$ $cm^{-2}$ (top) or $3 \times 10^{16}$ $cm^{-2}$ (bottom) $Ni^+$ ions and annealed at 700 °C.

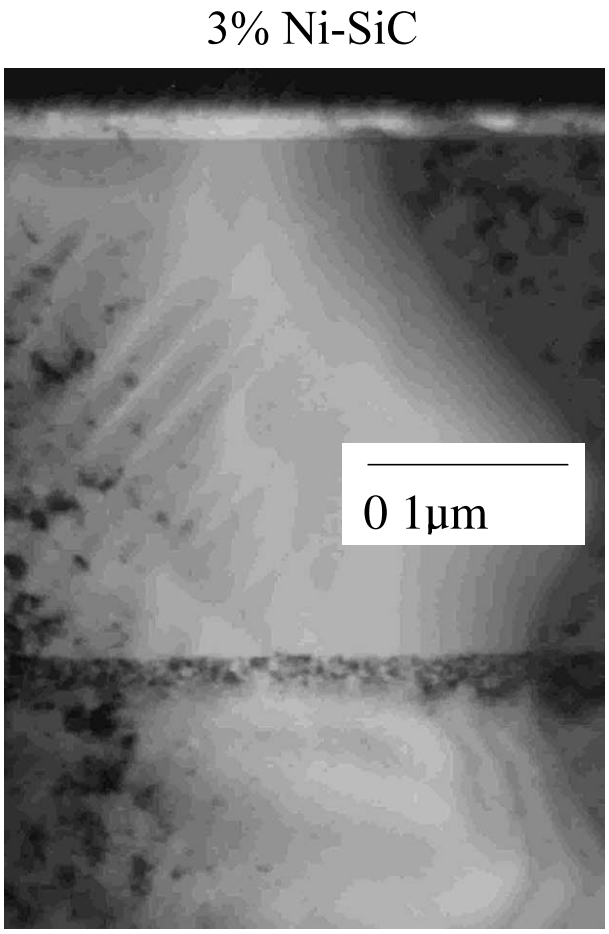


Fig. 4. TEM cross-section from SiC implanted with $3 \times 10^{16}$ cm$^{-2}$ $Ni^{+}$ ions at 250 keV and annealed at 700 °C.

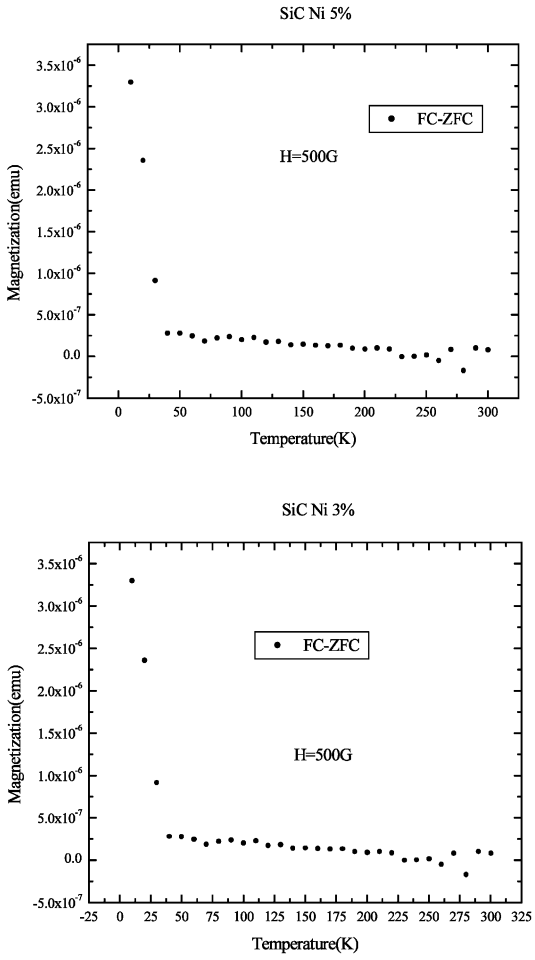


Fig. 5. Temperature dependence of difference between field-cooled and zero field-cooled magnetization from SiC implanted with either $5 \times 10^{16}$ cm$^{-3}$ (top) or $3 \times 10^{16}$ cm$^{-3}$ (bottom) $Ni^{+}$ ions and annealed at 700 °C.

potential phases that could form in this material. The non-hexagonal phases would lead to new symmetries in the diffraction pattern, while the hexagonal phases would produce satellite spots. Neither of these cases is observed experimentally.

Fig. 3 shows the temperature dependence of the difference in magnetization signal between field-cooled and zero field-cooled conditions at a field of 500 G for the 5% (top) and 3% (bottom) Ni-implanted GaN annealed at 700 °C. In both cases there is a sharp transition at $\leq 50$ K due to a ferromagnetic contribution to the magnetization. The large paramagnetic background has been subtracted in both plots. The result that Ni does not produce high transition temperatures in GaN will be an important input into existing theories of carrier-induced magnetism in semiconductors.[10,11,19] The decreasing signal that exists from $\sim 50$ to 250 K in Fig. 3 (bottom) may originate from superparamagnetic clusters of GaNi that are present with size below the 20 Å resolution of TEM.

Fig. 4 shows a TEM cross-sectional micrograph from a 3 at.% Ni-implanted SiC sample after 700 °C annealing. There is a defect band $\sim 17$ nm wide formed at the end-of-range of the Ni ions and at a depth of $\sim 0.26$ μm from the surface. The SADP from the implanted region did not show any significant differences from the control material, indicating that none of the potential secondary phases listed in Table 1(b) formed in our samples.

The temperature-dependent magnetization data (field cooled minus zero field cooled signal) from 5 at.% (top) and 3 at.% (bottom) SiC samples is shown in Fig. 5. As with the GaN, there are sharp transitions indicating the presence of ferromagnetic contributions at $\leq 50$ K. This is considerably lower than the 175 K found for Fe-implanted SiC and indicates that Ni-doping will not be useful in producing room temperature ferromagnetism in the material.

## 4. Summary and conclusions

High doses of Ni implanted into GaN and SiC produce ferromagnetic contributions to the magnetization that are present at $\leq 50$ K. There are no other

phases present in either material, at least to the sensitivity of TEM and SADP. The origin of the ferromagnetism is not clear in either material since the carrier density in both is expected to be too low to produce carrier-induced magnetism. Our result for Ni in GaN is similar to results for Fe incorporated in GaN during molecular beam epitaxy [8]. Future work should focus on determining the bandgap and carrier density dependence of the transition temperatures, perhaps by implanting Ni into $In_xGa_{1-x}N$ and $Al_xGa_{1-x}N$.

## Acknowledgements

The work at UF is partially supported by NSF-DMR 0101438 (V. Hess) while that of RGW is partially supported by ARO.

## References

[1] G.A. Prinz, Science 282 (1998) 1660.
[2] J. de Boeck, G. Borghs, Phys. World 12 (1999) 27.
[3] D.D. Awschalom, J.M. Kikkawa, Phys. Today 52 (1999) 33.
[4] B.T. Jonker, Y.D. Park, B.R. Bennett, H.D. Cheong, G. Kioseoglou, A. Petrou, Phys. Rev. B62 (2000) 8181.
[5] Y. Ohno, D.K. Young, B. Bescholen, F. Matsukura, H. Ohno, D.D. Awschalom, Nature 402 (1999) 790.
[6] Y.D. Park, B.T. Jonker, B.R. Bennett, G. Itkos, M. Furis, G. Kioseoglou, A. Petrou, Appl. Phys. Lett. 77 (2000) 3989.
[7] H. Ohno, J. Mag. Magn. Mater. 200 (1999) 110.
[8] H. Akinaga, S. Nemeth, J. de Boeck, L. Nistor, H. Bender, G. Borghs, H. Ofuchi, M. Oshima, Appl. Phys. Lett. 77 (2000) 4377.
[9] H. Ohno, D. Chiba, F. Matsukura, T. Omiya, E. Abe, T. Dietl, Y. Ohno, K. Ohtani, Nature 408 (2000) 944.
[10] T. Dietl, H. Ohno, F. Matsukura, J. Cibert, D. Ferrand, Science 287 (2000) 1019.
[11] K. Sato, H. Katayama-Yoshida, Jpn. J. Appl. Phys. 39 (2000) L255.
[12] N. Theodoropoulou, A.F. Hebard, M.E. Overberg, C.R. Abernathy, S.J. Pearton, S.N.G. Chu, R.G. Wilson, Appl. Phys. Lett. 78 (2001) 3475.
[13] N. Theodoropoulou, K.P. Lee, M.E. Overberg, S.N.G. Chu, A.F. Hebard, C.R. Aberrantly, S.J. Pearton, R.G. Wilson, J. Nanoscience Nanotech. 1 (2001) 101.
[14] S.O. Kucheyev, J.E. Bradley, J.S. Williams, C. Jagadish, M.V. Swain, G. Li, Appl. Phys. Lett. 78 (2001) 156.
[15] S.O. Kucheyev, J.S. Williams, C. Jagadish, J. Zou, G. Li, Phys. Rev. B 62 (2000) 7510.
[16] S.O. Kucheyev, S.J. Williams, S.J. Pearton, Mater. Sci. Eng. R33 (2001) 51.
[17] S.J. Pearton, F. Ren, A.P. Zhang, K.P. Lee, Mater. Sci. Eng. R30 (2000) 55.
[18] V. Wahl, A. Vantomme, G. Langouche, J.G. Correia, L. Peralta, Appl. Phys. Lett. 78 (2001) 3217.
[19] J. Schliemann, J. Koniz, H.H. Lin, A.H. McDonald, Appl. Phys. Lett. 78 (2001) 1550.